Supporting Information

Lead-free, formamidinium germanium-antimony halide ($FA_4GeSbCl_{12}$) double perovskite solar cells: effect of band offsets

Karthick Sekar,[a,b,*] Latha Marasamy,[c] Sasikumar Mayarambakam,[d,*] Hesham Hawashin,[a] Mohamad Nour,[b] Johann Bouclé[a]

(a) Univ. Limoges, CNRS, XLIM, UMR 7252, F-87000, Limoges, France.
(b) GREMAN UMR 7347, Université de Tours, CNRS, INSA Centre Val de Loire, 37071 Tours, France.
(c) Facultad de Química, Materiales-Energía, Universidad Autónoma de Querétaro, Santiago de Querétaro, Querétaro, C.P. 76010, Mexico.
(d) Department of Chemistry, Indian Institute of Science Education and Research (IISER)-Tirupati, Tirupati, 517507, A.P., India.

Table S1. SCAPS-1D input parameters of FTO, TiO_2, $FA_4GeSbCl_{12}$ and Cu_2O.

Parameters	**FTO (TCO)**	**TiO_2 (ETL)**	**$FA_4GeSbCl_{12}$ (Absorber)**	**Cu_2O (HTL)**
Thickness (nm)	500	30	300	100
Bandgap, E_g (eV)	3.50	3.20	1.3	2.17
Affinity, χ (eV)	4.00	3.9	3.50	3.2
Permittivity, ε_r	9.00	9.00	2.59	7.11
Effective density of states at CB, N_c (cm^{-3})	2.2×10^{18}	2.2×10^{18}	2.2×10^{18}	2.02×10^{17}
Effective density of states at VB, N_v (cm^{-3})	1.8×10^{19}	1.8×10^{19}	2.0×10^{18}	1.1×10^{19}
Mobility of electrons, μ_n ($cm^2V^{-1}s^{-1}$)	20	20	2268	200
Mobility of holes, μ_p ($cm^2V^{-1}s^{-1}$)	10	10	478	80
Density of n-type doping, N_D (cm^{-3})	1.0×10^{18}	1.0×10^{19}	0	0
Density of p-type doping, N_A (cm^{-3})	0	1	1.0×10^{15}	1.0×10^{18}
Density of defects, N_t (cm^{-3})	1.0×10^{15}	1.0×10^{15}	1.0×10^{16}	1.0×10^{15}
Reference	1	2,3	4,5	2,6

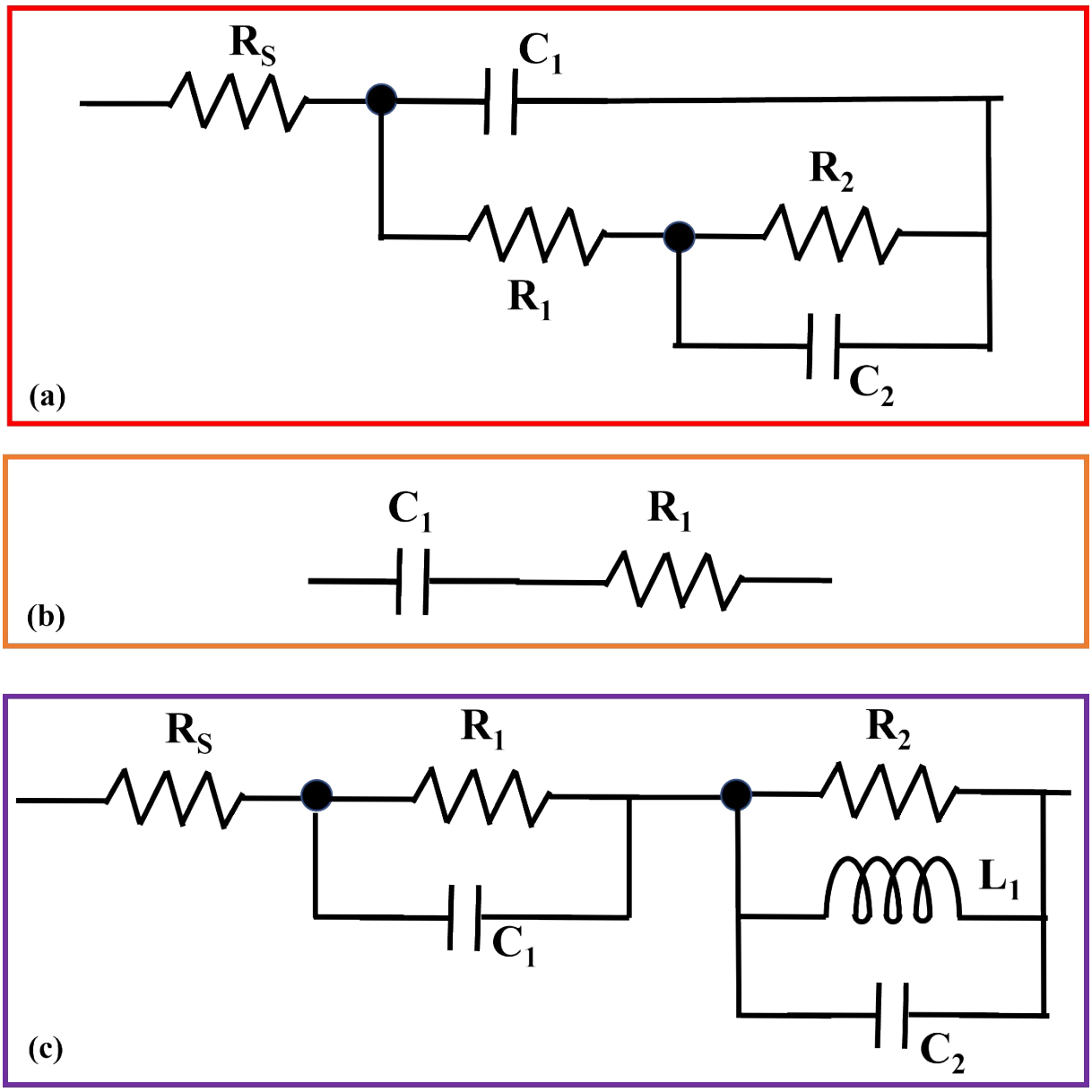

Figure S1. Equivalent circuit for Nyquist plots of EIS spectra with respect to the SCAPS-1D impedance data under AM 1.5 spectrum. (a) CBO (- 0.4 eV, 0 eV, + 0.2 eV), VBO (+ 0.57 eV), N_t (1E14 cm^{-3}, 1E18 cm^{-3}, 1E20 cm^{-3}) and absorber thickness (200 nm), (b) VBO (- 0.4 eV and 0 eV), and (c) absorber thickness (1000 nm and 3000 nm), 1000 nm (0 V, 0.3 eV, 0.6 eV), Series resistance (0.2 Ω.cm^2, 1.4 Ω.cm^2, 2.5 Ω.cm^2) and Shunt resistance (1k Ω.cm^2, 50k Ω.cm^2, 200k Ω.cm^2), respectively.

Table S2. Fitted results from the Nyquist Plot of simulated solar cell with different selected parameters (CBO, VBO, N_t, absorber thickness, bias voltage, series and shunt resistances).

		Rs $\Omega.cm^2$	L	R $\Omega.cm^2$ (HF)	CPE or C F/cm^2 (HF)	R $\Omega.cm^2$ (LF)	CPE or C F/cm^2 (LF)	tau (LF)
CBO (eV)	**- 0.4**	0.004		451	6.403E-9	228	1.341E-5	0.0031
	0	0.004		617	6.570E-9	9552	3.512E-6	0.0336
	+ 0.2	0.004		739	6.566E-9	37041	2.812E-6	0.1042
VBO (eV)	**- 0.4**					0.0195	2.751E-5	5.3745E-7
	0					0.014	3.346E-5	4.6840E-7
	+0.57	0.045		618	6.562E-9	9554	3.512E-6	0.0336
Nt (cm^{-3})	**E14**	0.066		53.45	6.606E-9	10100	4.406E-6	0.0445
	E18	0.044		53.31	6.604E-9	4889	4.437E-6	0.0217
	E20	0.044		40	6.557E-9	85.71	8.531E-6	7.3115E-4
Absorber Thickness (nm)	**200**	0.051		20	9.85E-9	9172	1.196E-5	0.1097
	1000	0.041	0.478	11006	4.32E-9	2035	1.718E-8	3.4969E-5
	3000	0.046	0.505	10327	4.39E-9	2131	1.722E-8	3.6706E-5
1000 (nm)	**0 V**	0.041	0.478	11006	4.32E-9	2035	1.718E-8	3.4969E-5
	0.3 V	0.041	0.333	6738	5.42E-9	1525	1.872E-8	2.8552E-5
	0.6 V	0.039	0.018	372	7.46E-9	99.63	2.948E-8	2.9371E-6
R_{series} ($\Omega.cm^2$)	**0.2**	0.241	0.477	11006	4.315E-9	2031	1.726E-8	3.5053E-5
	1.4	1.442	0.477	11005	4.313E-9	2029	1.730E-8	3.5104E-5
	2.5	2.543	0.473	11004	4.273E-9	1996	1.797E-8	3.5878E-5
R_{shunt} ($\Omega.cm^2$)	**1k**	0.044	0.0026	917	3.498E-9	10.93	2.716E-7	2.9688E-6
	50k	0.044	0.3000	9029	4.074E-9	1276	2.267E-8	2.8924E-5
	200k	0.041	0.4217	10419	4.145E-9	1724	2.063E-8	3.5571E-5

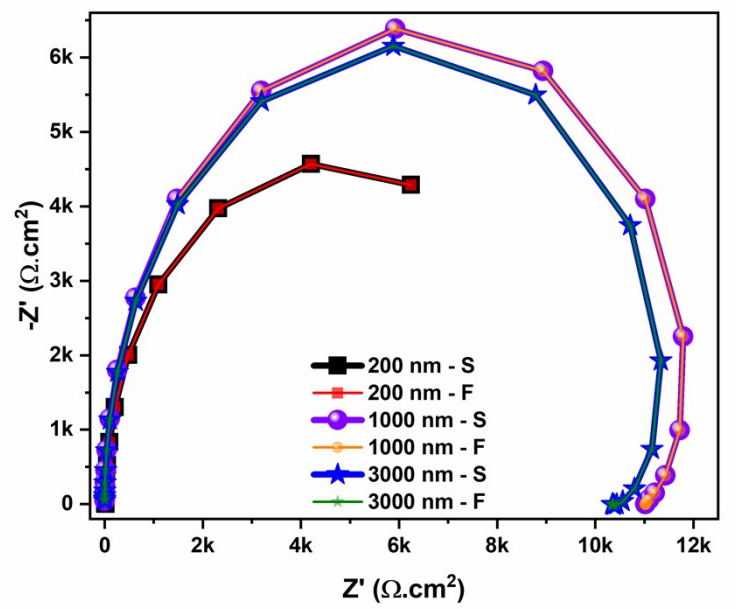

Figure S2. Nyquist plots as a function of absorber thicknesses. Note: S signifies the SCAPS impedance data, and F denotes fitted data.

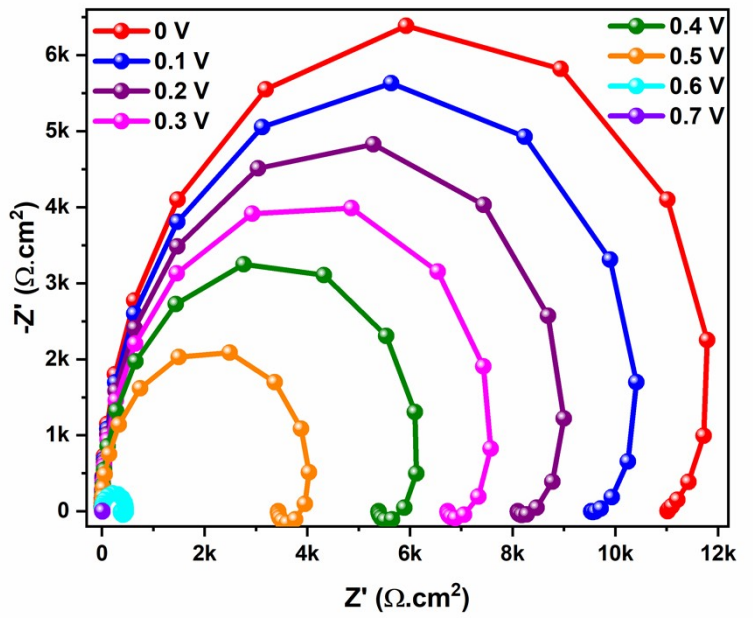

Figure S3. Nyquist plots of solar cell with 1000nm absorber thickness measured at different bias voltage from 0 to 0.7 V.

Table S3. SCAPS-1D input parameters of FTO, TiO_2, en-$FASnI_3$ and PTAA.

Parameters	**FTO (TCO)**	**TiO_2 (ETL)**	**en-$FASnI_3$ (Absorber)**	**PTAA (HTL)**
Thickness (nm)	500	30	300	100
Bandgap, E_g (eV)	3.50	3.20	1.9	2.96
Affinity, χ (eV)	4.00	3.9	3.520	2.3
Permittivity, ε_r	9.00	9.00	8.20	9
Effective density of states at CB, N_c (cm^{-3})	2.2×10^{18}	2.2×10^{18}	2.2×10^{18}	2.0×10^{21}
Effective density of states at VB, N_v (cm^{-3})	1.8×10^{19}	1.8×10^{19}	2.0×10^{18}	2.0×10^{21}
Mobility of electrons, μ_n ($cm^2V^{-1}s^{-1}$)	20	20	22	1
Mobility of holes, μ_p ($cm^2V^{-1}s^{-1}$)	10	10	22	40
Density of n-type doping, N_D (cm^{-3})	1.0×10^{18}	1.0×10^{19}	0	0
Density of p-type doping, N_A (cm^{-3})	0	1	7.0×10^{16}	1.0×10^{18}
Density of defects, N_t (cm^{-3})	1.0×10^{15}	1.0×10^{15}	2.0×10^{15}	1.0×10^{15}
Reference	[1]	[2,3]	[7–9]	[6,9]

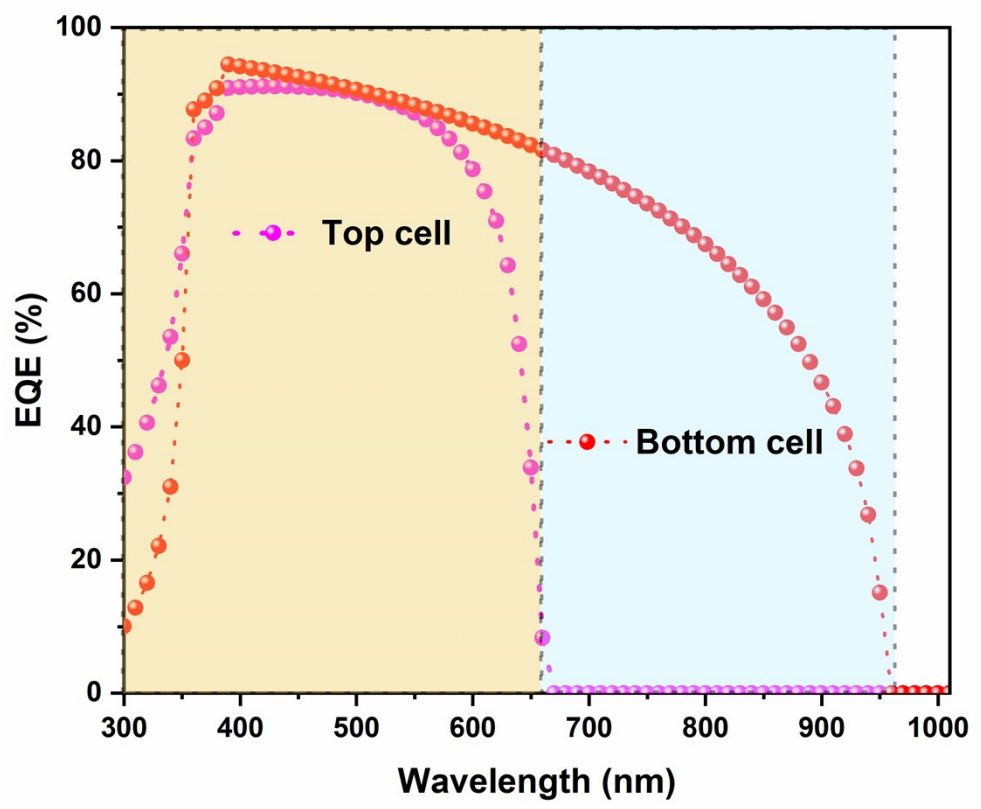

Figure S4. EQE of top and bottom cells.

References

1 S. Karthick, S. Velumani and J. Bouclé, *Sol. Energy*, , DOI:10.1016/j.solener.2020.05.041.

2 A. A. Kanoun, M. B. Kanoun, A. E. Merad and S. Goumri-Said, *Sol. Energy*, 2019, **182**, 237–244.

3 A. U. Duha and M. F. Borunda, *Opt. Mater. (Amst).*, 2022, **123**, 111891.

4 C. Walkons, R. Murshed and S. Bansal, *Sol. RRL*, 2020, **4**, 2000299.

5 W. B. Dai, S. Xu, J. Zhou, J. Hu, K. Huang and M. Xu, *Sol. Energy Mater. Sol. Cells*, 2019, **192**, 140–146.

6 S. Karthick, J. Bouclé and S. Velumani, *Sol. Energy*, 2021, **218**, 157–168.

7 W. Ke, C. C. Stoumpos, M. Zhu, L. Mao, I. Spanopoulos, J. Liu, O. Y. Kontsevoi, M. Chen, D. Sarma, Y. Zhang, M. R. Wasielewski and M. G. Kanatzidis, *Sci. Adv.*, , DOI:10.1126/sciadv.1701293.

8 S. Abdelaziz, A. Zekry, A. Shaker and M. Abouelatta, *Opt. Mater. (Amst).*, , DOI:10.1016/j.optmat.2020.109738.

9 T. Yokoyama, Y. Nishitani, Y. Miyamoto, S. Kusumoto, R. Uchida, T. Matsui, K. Kawano, T. Sekiguchi and Y. Kaneko, *ACS Appl. Mater. Interfaces*, 2020, **12**, 27131–27139.